BULLETIN OF THE CHEMICAL SOCIETY OF JAPAN VOL. 39 2588—2597 (1966)

The Quenching Action of Benzoic Acid and Methylbenzoate on the Fluorescence of Naphthalene Derivatives. III.
The Solvent Effect on the Quenching of the Fluorescence of Dimethylnaphthylamine by Methylbenzoate

By Takuji MIWA and Masao KOIZUMI

Department of Chemistry, Faculty of Science, Tohoku University, Katahira-cho, Sendai

(Received April 15, 1966)

The fluorescence and absorption spectra and the quenching of the fluorescence of *N, N*-dimethyl-2-naphthylamine by methylbenzoate have been measured in cyclohexane, benzene, *p*-dioxane, isopropyl ether, ethyl ether, ethyl acetate, tetrahydrofuran, acetone and *N, N*-dimethylformamide (in the order of DK values). The fluorescence and the absorption spectra show a red-shift with the polarity of the solvent. By the method of Lippert and Mataga, the dipole moment of the excited fluorescer molecule has been estimated to be 4.1D. In nonpolar and weakly polar solvents, the methyl benzoate-added systems give fluorescence spectra with a swell or a shoulder on the long wavelength side, but this does not occur in *N, N*-dimethylformamide. When methyl benzoate is used as the solvent, two peaks of fluorescence are observed. The new emission has been interpreted as a charge-transfer emission, and the temperature-dependence of the fluorescence spectra has led to the conclusion that an encounter of fluorescent and quencher molecules is prerequisite for the appearance of CT emission. The quenching efficiencies in different solvents have been dealt with in reference to that in *N, N*-dimethylformamide, since the quenching in this solvent has been found to be almost encounter-controlled. A general correlation has been found between the quenching efficiency and the polarity of the solvent. The quenching mechanism and also the appearance of the CT emission have been discussed.

In previous papers,[1] the quenching action of benzoic acid and its ester on the fluorescence of some naphthalene derivatives was discussed from the viewpoint of a charge transfer (CT) mechanism. Most of the results were favorable to this

---

[1] T. Miwa and M. Koizumi, This Bulletin, **38**, 529 (1965).

viewpoint, but there was no conclusive evidence. The purpose of the present paper is to give further evidence for the CT mechanism of the quenching action of methyl benzoate (MB) on *N*, *N*-dimethyl-2-naphthylamine (DMNA) by studying the solvent effect on the fluorescence spectra and on the quenching action.

Weller was the first to offer confirmative evidence for the CT mechanism of quenching. Leonhard and Weller,$^{2)}$ for instance, studied the quenching action of aniline, *N*, *N*-dimethylaniline, etc., on the fluorescence of perylene and found that the efficiency of quenching depends largely on the polarity of the solvent; for example, it is large in acetonitrile, but quite small in benzene. They also found that a new emission due to a CT complex between fluorescer and quencher is observable only in nonpolar solvents. Further, by means of a flash technique, they succeeded in detecting the radical anion of perylene in polar solvents, whereas only the enhancement of the T–T absorption was observed in nonpolar solvents. Mataga et al.$^{3)}$ extended such studies using similar systems. These works led us to expect analogous phenomena in the system of DMNA and MB; we have found that this is really true. Besides, we have ascertained the dipole moment of the excited DMNA by employing the method of Mataga and Lippert.$^{4)}$

Experimental

Material.—Acetone of Wako Junyaku, G. R. grade, was stored over potassium permangnate for 3 days, boiled for 2 hr., and then, after distillation, dried over potassium carbonate and finally fractionated. The middle half (b. p. 56.5°C) was used. Ethyl acetate was kept over anhydrous potassium carbonate and then fractionated carefully. Ethyl ether and isopropyl ether of Kanto Kagaku, G. R. grade, were treated with a 10% solution of sodium carbonate for 24 hr. and then dehydrated with anhydrous calcium chloride and finally with sodium. The ethers were repeatedly decanted, and fresh sodium was added until no hydrogen evolved. They were then distilled slowly over sodium. Tetrahydrofuran of Kanto Kagaku, G. R. grade, was repeatedly treated with fresh sodium and decanted until the evolution of hydrogen stopped. It was then distilled over sodium. Methyl benzoate, E. P. grade, was washed with a concentrated aqueous solution of potassium carbonate and dried over anhydrous pottassium carbonate and then over anhydrous mangesium sulfate. After being distilled under reduced pressure, it was passed through 1-meter silica gel column and then distilled in vacuo. The sample thus purified showed no impurity luminescence when the excitation wavelength is longer than 320 mμ. *p*-dioxane, benzene and cyclohexane were purified in the same way as in a previous paper.$^{1)}$

Procedure.—The absorption spectra were measured with a Hitachi ESP III recording spectrophotometer. The fluorescence and action spectra were measured with an Aminco-Bowman spectrofluorimeter. The samples were usually not degassed. The temperature was maintained at 25°C. Some measurements were made at low temperatures down to the liquid nitrogen temperature. The concentration of *N*, *N*-dimethyl-2-naphthylamine was always 10^{-4} M. The excitation wavelength was usually 350 mμ. In dealing with the intensity data, the peak intensities were used without any correction for the spectral sensitivity of the instrument. The solvent effect on the optical density at the exciting wavelength, which was usually very small, was taken into account.

Results

The Solvent Effects on the Absorption and Fluorescence Spectra of DMNA in the Absence and in the Presence of MB.—The absorption spectra show a red shift and become broader as the polarity of the solvent increases. The addition of MB has a similar effect, the magnitude of which decreases with the increase in the polarity of the solvent.

In Table I some of the data on the absorption spectra are tabulated. Most of them will be used in the discussion below.

The solvent effects and the effect of the addition of MB on the fluorescence spectra of DMNA are

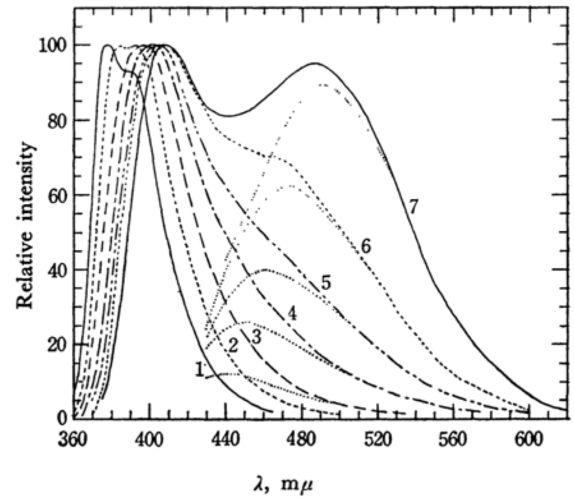

Fig. 1. Fluorescence spectra of DMNA-MB in cyclohexane.
MB: 1) 0, 2) 0.198, 3) 0.793, 4) 2.38, 5) 3.97, 6) 5.55, 7) 7.93 M (no cyclohexane)
dotted line, emission of the longer wavelength component (see text)

---

2) H. Leonhardt and A. Weller, *Z. physik. Chem., N. F.*, **29**, 277 (1961); *Ber. Bunsges. phys. Chem.*, **61**, 791 (1963).

3) N. Mataga, K. Ezumi and G. Takahashi, Symposium on Photochemistry, Tokyo (1964); N. Mataga and K. Ezumi, Symposium on Molecular Structure, Nagoya (1965); N. Mataga and M. Okada, ibid.

4) N. Mataga, Y. Kaifu and M. Koizumi, This Bulletin, **29**, 465 (1956); E. Lippert, *Z. Elektrochem.*, **61**, 962 (1957).

TABLE I. ABSORPTION SPECTRA DATA FOR DMNA IN THE ABSENCE AND IN THE PRESENCE OF MB

	Solvent	[DMNA] M	In the Absence of MB					In the presence of MB		
			λ_{max}. of the first abs. band mμ	λ_{max} of the second abs. band mμ	op.d. at 350 mμ (d)	Oscillator strength for the first abs. band (f_i)	$\frac{(f/n_D)_i}{(f/n_D)_9}$	λ_{max} of the first abs. band [MB]: 0.801	[MB]: 1.60	[MB]: 2.40
1)	Cyclohexane	1.00×10^{-4}	351.5	287.0, 297.6	0.287	0.039	0.84	352.5	352.5	353.5
2)	Benzene	1.00×10^{-4}	356.6	290.6, 300.6	0.294	0.050	1.03	356.5	356.5	357.5
3)	*p*-Dioxane	1.12×10^{-4}	355	289.0, 299.1	0.319	0.047	1.03	355	355	356
4)	Isopropyl ether	1.00×10^{-4}	352	287.4, 297.2	0.284	0.045	1.03	352	353	354
5)	Ethyl ether	1.00×10^{-4}	352	287.3, 297.3	0.294	0.046	1.06	352	353	
6)	Ethyl acetate	1.00×10^{-4}	354	288.0, 297.9	0.288	0.047	1.06	354	354	354.5
7)	Tetrahydrofuran	1.00×10^{-4}	354.5	289.0, 298.8	0.292	0.053	1.16	355	355	355.5
8)	Acetone	1.00×10^{-4}	355	—	0.280	0.049	1.13	355	355	355
9)	*N, N*-Dimethylformamide	1.00×10^{-4}	357	290.0, 299.5	0.287	0.046	1.00	357	357.5	358
10)	Methyl benzoate	1.00×10^{-4}	358	—	0.281	0.054	1.13	—	—	—

TABLE II. SOME CHARACTERISTICS OF THE EMISSION SPECTRA FOR THE DMNA-MB SYSTEM

	Solvent	[DMNA] M$\times10^4$	In the absence of MB			In the presence of MB			
						[MB] : 0.801 M		[MB] : 2.40 M	
			λ_{max} of the fluorescence spectra mμ	F_{0i}/F_{09}	$\alpha_i\equiv\left(\frac{F_{0i}}{F_{09}}\right)\left(\frac{d_9}{d_i}\right)$	λ_{max} of the s. flu.	λ_{max} of the l. flu.	λ_{max} of the s. flu.	λ_{max} of the l. flu.
1)	Cyclohexane	1.00	379	0.720	0.720	396		401	450±2
2)	Benzene	1.00	395	0.865	0.844	398		403	470±4
3)	*p*-Dioxane	1.12	400	1.24	1.12	404		406	478±5
4)	Isopropyl ether	1.00	390	0.467	0.472	398		404	467±3
5)	Ethyl ether	1.00	393	0.671	0.655	401			467±3*
6)	Ethyl acetate	1.00	402	0.654	0.652	404		407	480±7
7)	Tetrahydrofuran	1.00	403	0.819	0.805	405		406	485±5
8)	Acetone	1.00	409	0.645	0.661	410		411	505±10
9)	*N, N*-Dimethylformamide	1.00	412	1.00	1.00	413		413	
10)	Methyl benzoate	1.00	406, 490	0.00260	0.00266				

*[MB], 1.60 M

TABLE III. THE DATA FOR THE CALCULATION OF THE DIPOLE MOMENT OF EXCITED DMNA

	Solvent	$\tilde{\nu}_{a\ max}$ cm^{-1}	$\tilde{\nu}_{f\ max}$ cm^{-1}	$\tilde{\nu}_{a\ max}-\tilde{\nu}_{f\ max}$ cm^{-1}	ε at 25°C	n_D at 25°C	μ (D)	η (cpoise) at 25°C
1)	Cyclohexane	28450	26390 (27700)*	2060	2.020	1.4274	0	0.898
2)	Benzene	28050	25320	2730	2.273	1.4980	0	0.6028
3)	*p*-Dioxane	28170	25000	3170	2.280	1.42025	0.45	1.16
4)	Isopropyl ether	28410	25640	2770	3.88	1.36618	1.22	0.379
5)	Ethyl ether	28410	25450	2960	4.335 (20°C)	1.35272 (20°C)	1.15	0.233
6)	Ethyl acetate	28250	24880	3370	6.02	1.36979	1.81	0.421
7)	Tetrahydrofuran	28210	24810	3400	7.39	1.40355	1.68	0.51 (20°C)
8)	Acetone	28170	24450	3720	20.70	1.35609	2.72	0.305
9)	*N, N*-Dimethylformamide	28010	24270	3740	36.71	1.4269	3.86	0.908
10)	Methyl benzoate	27930	24630	3300	6.548	1.4961	1.86	1.846

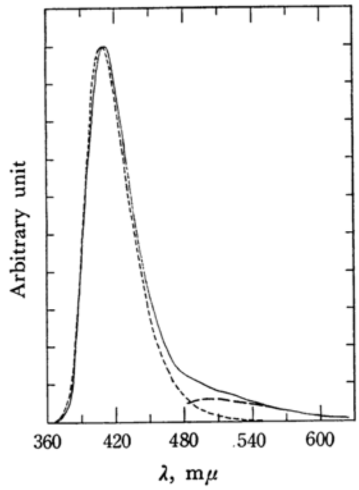

Fig. 2. Fluorescence spectra of DMNA-MB in acetone.

---- DMNA (1×10^{-4} M) in acetone
—— DMNA (1×10^{-4} M) + MB (2.40 M) in acetone
— — Emission of the longer wavelength component

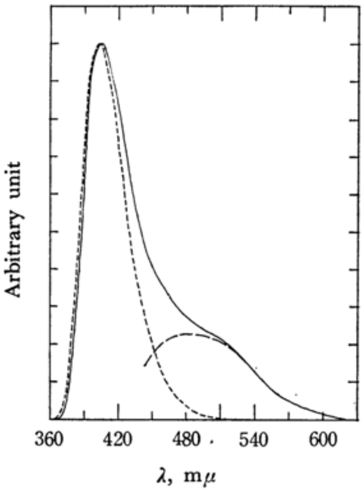

Fig. 3. Fluorescence spectra of DMNA-MB in ethyl acetate.

---- DMNA (1×10^{-4} M) in ethyl acetate
—— DMNA (1×10^{-4} M) + MB (2.40 M) in ethyl acetate
— — Emission of the longer wavelength component

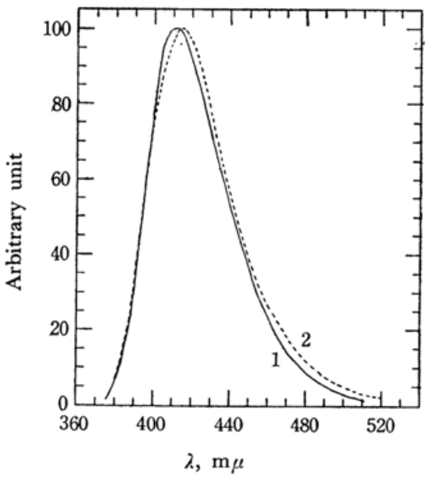

Fig. 4. Fluorescence spectra of DMNA-MB in dimethylformamide.

1) DMNA (1×10^{-4} M) in dimethylformamide
2) DMNA (1×10^{-4} M) + MB (2.40 M) in dimethylformamide

similar to those on the absorption spectra, but more pronounced. As for the latter effect, it is remarkable in cyclohexane, but very small in dimethylformamide. A notable finding is that the tail in the long-wavelength side grows gradually with the addition of MB, and in most solvents a shoulder and, in favorable cases, a new peak comes to be observed. This phenomenon is observed easily in less polar solvents. In *N*, *N*-dimethylformamide, which is the most polar solvent in the present experiment, the above change is very weak. When 10^{-4} M DMNA is dissolved in pure MB, there exist two emission bands, with peaks at 406 mμ and 490 mμ. These two peaks are about the same height, but the integrated intensity for the latter is much larger because of its broad shape. The real difference is probably still larger in view of the spectral sensitivity of the photometer. Some typical examples of the fluorescence spectra are shown in Fig. 1—4, where the peak height of the short-wavelength emission is normalized to unity. The real intensity decreases with the increase in the MB concentration. It may be seen that the solvent effect on the new emission is much larger.

To make sure that this new emission is not due to any impurity which might be present in MB, the excitation spectra were taken on various systems and at various wavelengths of emission spectra. The results confirmed that the new band originates from the light absorption of DMNA, since the excitation spectra agreed quite well with the absorption spectra of DMNA. In Table II some characteristic data on the emission spectra are tabulated. The relative intensities of fluorescence with reference to *N*, *N*-dimethylformamide as the solvent, (F_{0i}/F_{09}), and the relative quantum efficiencies, $(F_{0i}/F_{09})\times(d_9/d_i)_{350}$, where d_i is the optical density in solvent i at 350 mμ (the suffix, 0, indicates the non-existence of MB), are listed since they will be useful for the later discussion. The peak position of the longer-wavelength emission was evaluated by subtracting the shorter-wavelength emission from the total. Since this procedure involves some arbitrariness, however, the data given are not very reliable.

The Dipole Moment of the Excited DMNA.—Since the absorption and emission spectra in various solvents have been measured, the dipole moment of the excited DMNA molecule can be evaluated by means of the following formula:[4]

$$hc(\tilde{\nu}_a-\tilde{\nu}_f) = \frac{(\mu_e-\mu_g)^2}{a^3}\left[\frac{2(\varepsilon-1)}{2\varepsilon+1}-\frac{2(n_D^2-1)}{2n_D^2+1}\right] + \text{const.} + \text{small terms} \qquad (1)$$

The data necessary for the calculation are given in Table III.

The dipole moments and the viscosities of the solvents are listed so that they can be used in the later discussion. ε and n are the values at 25°C. The plot $\tilde{\nu}_a-\tilde{\nu}_f$ vs. $\{2(\varepsilon-1)/2(\varepsilon+1)-2(n_D^2-1)/(2n_D^2+1)\}$ is given in Fig. 5. Assuming a (the cavity radius in Onsager's theory) in Eq. 1 as ~3 Å, the value of $\mu_e-\mu_g$ was found to be 4.1D (Debye). This is reasonable in view of the values of 4.5D, 4.4D, and 3.5D reported for *N*, *N*-dimethyl-1-naphthylamine, 1-naphthylamine, and 2-naphthylamine by Mataga et al.[4] Thus it was confirmed that the excited state of DMNA is highly polar.

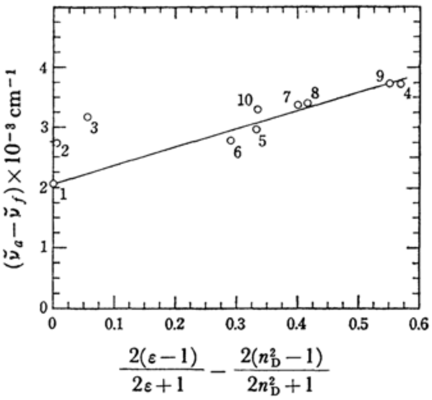

Fig. 5. Evaluation of the dipole moment of the excited DMNA.
Solvent: 1) cyclohexane, 2) benzene, 3) *p*-dioxane, 4) acetone, 5) ethyl ether, 6) isopropyl ether 7) ethyl acetate, 8) tetrahydrofuran, 9) *N*, *N*-dimethylformamide, 10) methyl benzoate

Intensity Relations on the Fluorescence of DMNA.—In all the solvents, the fluorescence intensities of DMNA decrease upon the addition of MB. In Figs. 6, 7, and 8, the values of $(F_{0i}d_i/F_id_{0i})-1$ are plotted against the MB concentrations. Since all the plots deviate more or less from the Stern-Volmer relation with the increase in the concentration of the quencher, the quenching constants, K_A, in terms of this equation were evaluated from the slopes of the curves at the point of origin. They are given in Table IV, along with the values obtained from the $(F_{0i}d_i/F_id_{0i})-1$ values at 0.160 and 0.801 M concentrations of MB (K_B and K_C). The moderate agreement of the K_A, K_B and K_C values assures the reliability of the data.

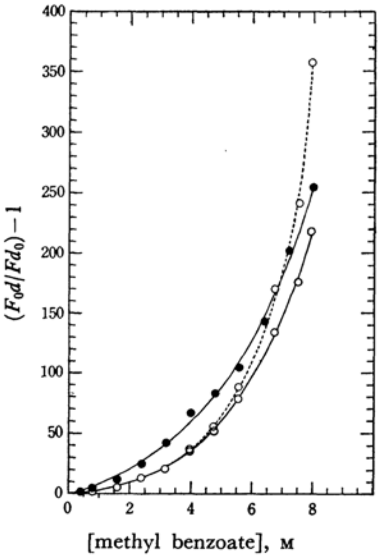

Fig. 6. $(F_{0i}/F_i)(d_i/d_{0i})-1$ vs. [MB] plot for
—○— , benzene solution;
—●— , cyclohexane solution (corrected for impurity luminescence in MB);
--○-- , cyclohexane solution (uncorrected).
(corrected values only are given in Figs. 7 and 8).

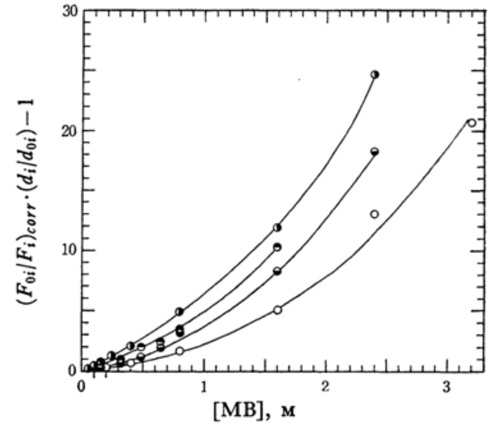

Fig. 7. $(F_{0i}/F_i)(d_i/d_{0i})-1$ vs. [MB] plot for
◑ benzene solution;
◓ ethyl ether solution;
◒ isopropyl ether solution;
○ cyclohexane solution;

When the concentrations of MB are 1.60, 2.40, and 3.20 M, a new emission band of the longer wavelength becomes notable in most cases. As a

Table IV. Intensity relation of the fluorescence

	Solvent	K_A	K_B	K_C	[MB] : 0.801 м			[MB] : 1.60 м		
					$\left(\frac{F_{0i}}{F_i}\right)\left(\frac{d_i}{d_{0i}}\right)-1$	$\frac{F_i}{F_{i500}}$	$\frac{F_0\left(\frac{d_i}{d_{0i}}\right)-F_i}{F_{i500}}$	$\left(\frac{F_{0i}}{F_i}\right)\left(\frac{d_i}{d_{0i}}\right)-1$	$\frac{F_i}{F_{i500}}$	$\frac{F_0\left(\frac{d_i}{d_{i0}}\right)-F_i}{F_{i500}}$
1)	Cyclohexane	1.7	1.6	2.1	1.70	24.4	41.6	5.10	13.3	68.0
2)	Benzene	5.2	5.1	6.1	4.85	17.5	85.0	11.9	8.80	105
3)	*p*-Dioxane	11	9.7	12	10.0	13.6	135	28.3	6.18	170
4)	Isopropyl ether	2.2	1.9	4.0	3.21	17.6	56.4	8.33	8.09	67.4
5)	Ethyl ether	3.9	4.8	4.4	3.47	14.4	49.9	10.3	7.41	75.5
6)	Ethyl acetate	24	23	28	22.1	12.9	285	45.7	6.61	302
7)	Tetrahydrofuran	25	25	29	23.2	10.8	253	52.8	6.84	366
8)	Acetone	64	59	65	52.5	26.0	1365	114	12.5	1419
9)	*N*, *N*-Dimethylformamide	72	69	93	74.1	25.6	1984	179	21.2	3779

Table V.

	Solvent	$Z_i=\frac{8\boldsymbol{R}T}{3000\,\varepsilon_i}$	$K_{cal}=Z_i\tau_0$	$\beta_i=d_i\frac{Z_i}{Z_9}$	$\frac{K_{Ai}}{K_{A9}}$	$\gamma_{Ai}=\frac{K_{Ai}}{K_{A9}\beta_i}$	$\frac{K_{Ci}}{K_{C9}}$	$\gamma_{Ci}=\frac{K_{Ci}}{K_{C9}\beta_i}$
1)	Cyclohexane	7.36×10^9	74	0.728	0.024	0.033	0.023	0.032
2)	Benzene	10.96×10^9	110	1.27	0.072	0.057	0.066	0.052
3)	*p*-Dioxane	5.70×10^9	57	0.874	0.15	0.17	0.13	0.15
4)	Isopropyl ether	17.43×10^9	174	1.13	0.031	0.027	0.043	0.038
5)	Ethyl ether	28.35×10^9	284	2.55	0.054	0.021	0.047	0.018
6)	Ethyl acetate	15.69×10^9	157	1.41	0.33	0.23	0.30	0.21
7)	Tetrahydrofuran	12.74×10^9	127	1.41	0.35	0.25	0.31	0.22
8)	Acetone	21.66×10^9	217	1.97	0.89	0.45	0.70	0.36
9)	*N*, *N*-Dimethylformamide	7.28×10^9	73	1.00	1.00	1.00	1.00	1.00

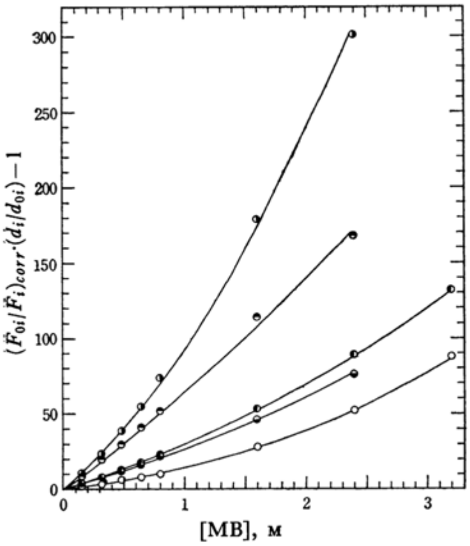

Fig. 8. $(F_{0i}/F_i)(d_i/d_{0i})-1$ vs. [MB] plot for
◑ *N*, *N*-dimethylformamide solution;
◓ acetone solution;
◐ tetrahydrofuran solution;
◒ ethyl acetate solution;
○ *p*-dioxane solution.
[DMNA], 1.12×10^{-4} м for *p*-dioxane
1.00×10^{-4} м for all the other solvents

measure of the intensities of this emission, $\{(F_{0i}d_i/d_{0i})-F_i\}/F_{i500}$ (F_{i500} is the fluorescence intensity at 500 mμ) and F_i/F_{i500} are listed in Table IV; for the sake of comparison, $(F_{0i}d_i/F_id_{0i})-1$ for the intrinsic emission of DMNA is also listed. The intensity at 500 mμ was used because the intensity at the peak is difficult to evaluate on account of the superposition of the two emission bands. It should be noted that the values of F_{i500} used as the measures of the new emission become more and more overestimated as the solvent polarity increases, because the solvent effect on this new emission is quite large. Thus, the data are only approximate in nature. However, a general tendency is observed for $\{(F_{0i}d_i/d_{0i})-F_i\}/F_{i500}$ to increase as the quenching constant K increases, whereas F_i/F_{i500} decreases at first, shows a minimum, and then increases again. Such tendencies may clearly be seen from Figs. 9 and 10 where $(F_0d_i/d_{0i}-F_i)/F_{i500}$ and F_{i500}/F_i are plotted, respectively against the concentration of MB. Moreover, Fig. 9 shows that the former quantity increases with the concentration of MB, while a comparison of Fig. 9 with Figs. 6, 7 and 8 indicates that the concentration effect on it is far less than on F_i. Figure 10 shows, on the other hand, that F_{i500}/F_i increases remarkably with the concentration of MB in most cases.

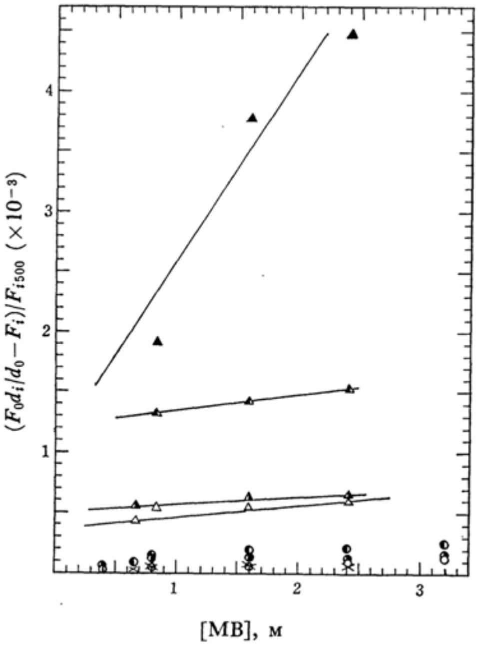

Fig. 9. $(F_0d_i/d_{0i}-F_i)/F_{i500}$ vs. [MB] plot for
○ cyclohexane, ◑ benzene, ◐ dioxane,
× isopropyl ether, △ ethyl acetate,
◭ tetrahydrofuran, ◮ acetone,
▲ *N N*-dimethylformamide.

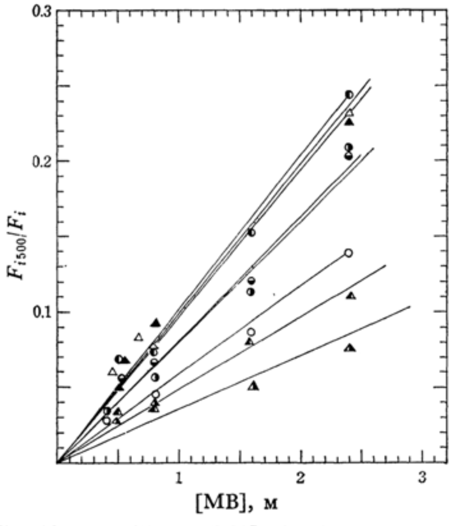

Fig. 10. F_{i500}/F_i vs. [MB] plot for
○ cyclohexane, ◑ benzene, ◐ dioxane,
◒ isopropyl ether, △ ethyl acetate,
▲ tetrahydrofuran, ◮ acetone,
◭ *N*, *N*-dimethylformamide.

The Effect of Temperature on the Fluorescence Spectra.—To make clear the nature of quenching as well as the origin of a new emission, the spectra were measured at different temperatures down to −182°C. The fluorescence spectra of DMNA 10^{-4} M in cyclohexane at this temperature is extremely sharp in comparison with those at room temperature. When 6.41 M of MB was added to the above solution, the intensity of the fluorescence at room temperature decreases remarkably and the spectra consist of the two emission bands with peaks at 406 and 486 mμ. At −182°C the emission consists of a single sharp band of a high intensity with a peak at 404 mμ. The shapes of the fluorescence spectra at different temperatures from −182°C up to −31°C are shown in Fig. 11. From the figure it may be seen that, at −31°C and at −38°C, there are two emission bands similar to those at room temperature. Although only one band occurs below −43°C, the tail in the longer wavelength gradually rises with the rise of temperature; the intensity decreases to some extent at −50°C. The intensities at −38°C and at −31°C are quite small.

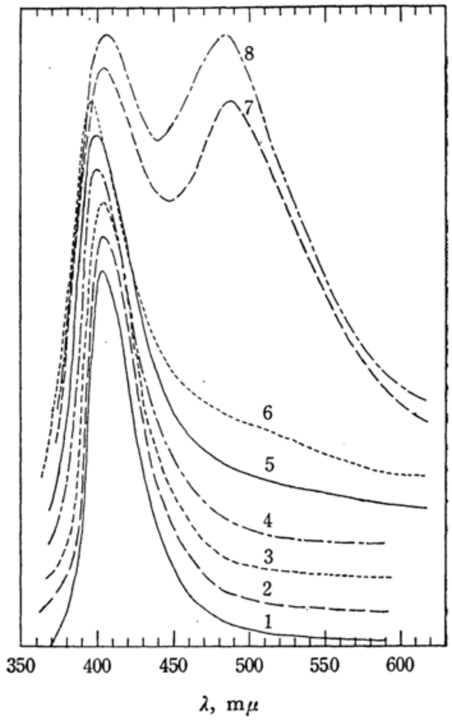

Fig. 11. Temperature dependence of the fluoressence spectra of DMNA-MB in cyclohexane.
[DMNA] : 1.00×10^{-4} M, [MB] : 6.41 M
temperature (°C): 1) −182, 2) −158, 3) −138, 4) −94, 5) −50, 6) −43, 7) −38, 8) −31
Intensity ratio of the normal fluorescence of DMNA : 8) 1, 7) 1.1, 6) 12, 5) 23, 4) 61, 3) 52, 2) 49, 1) 63

It should be noted that the above change proceeds as the sample melts. Thus the crystal begins to soften in appearance near −50°C, and around −43°C it partly begins to melt. At −38°C more than two-thirds of the crystals melts, until the melting ends at −31°C. The above observation leads to the conclusion that the quenching of the fluorescence is dynamic and, further, that a new emission arises from the encounter of an excited fluorescer molecule with a quencher molecule.

All the facts observed strongly support the view that the new emission is due to an excited CT complex. Hereafter, it will be designated as a CT emission.

Discussion

Since the quenching in the present investigation is dynamic in nature, the discussion can be made on the basis of a Stern-Volmer eq. of the following type:

$$\Phi_0/\Phi = F_0/F = 1 + \gamma Z\tau_0[\mathrm{Q}] = 1 + \frac{\gamma Z}{k_f}\Phi_0[\mathrm{Q}] \qquad (2)$$

where Φ and Φ_0 are the quantum yields of fluorescence in the presence and in the absence of the quencher. The experimentally-determined quenching constant, K_A, is:

$$K_\mathrm{A} = \frac{\gamma Z}{k_f}\Phi_0 \qquad (3)$$

where Z is the bimolecular rate constant for an encounter process and γ, the quenching efficiency for each encounter. Further, τ_0 and Φ_0 are written as follows:

$$\tau_0 = \frac{1}{k_f + k_d + k_{q02}[\mathrm{O}_2]} \qquad (4)$$

$$\Phi_0 = \frac{k_f}{k_f + k_d + k_{q02}[\mathrm{O}_2]} \qquad (5)$$

where k_f, k_d and $k_{q\mathrm{O}_2}$ are, respectively, the rate constants for emission, monomolecular deactivation, and bimolecular deactivation due to oxygen.

Now the Z value for each solvent can be estimated from the Stokes-Einstein formula, $8\boldsymbol{R}T/3000\,\eta$; the values are listed in Table V. $\tau_0 Z$ gives the quenching constant provided γ is unity. The values of $\tau_0 Z$ obtained by putting $\tau_0 = 10^{-8}$ sec. (estimated from the oscillator strength) are also given in the table (K_cal). A comparison of K_cal with K_A in Table IV will show that, in the case of N, N-dimethylformamide, they agree quite well. Of course, this is rather fortuitous, but there is no doubt that the quenching in this case is almost entirely diffusion-controlled. In all the other solvents, K_A is much less than K_cal. Therefore, it is appropriate to discuss the relative quenching efficiency with reference to $(Z\Phi_0/k_f)_9$ (9 is the numbering index for N, N-dimethylformamide). The relative quenching constant for solvent i is, then,

$$K_{Ai}/K_{A9} = (\gamma Z\Phi_0)_i/(Z\Phi_0)_9 = \frac{\gamma_i Z_i}{Z_9}\alpha_i = \gamma_i\beta_i \qquad \beta_i = \frac{Z_i}{Z_9}\alpha_i \qquad (6)$$

by assuming that $k_{f9} = k_{fi}$. This is approximately correct since the values of $(f/n_D)_i/(f/n_D)_9$ given in Table I are unity within +10% (except cyclohexane). The values for $\alpha_i = \Phi_{0i}/\Phi_{09}$ are given in Table II. The quenching efficiency for solvent i can, thus, be calculated from:

$$\gamma_i = \frac{K_{Ai}}{K_{A9}\beta_i}$$

The values of β_i, K_{Ai}/K_{A9} and γ_{Ai} are tabulated in Table V. The analogous quantities on the basis of K_C are also given to make sure that the values of γ_{Ci} thus obtained are quite reliable for comparing the quenching efficiency. Figure 12 shows the plot of γ_i and $\{(F_{0i}d_i/d_{0i}\alpha_i) - F_i\}/F_{i500}$ against the dipole moments (μ) of the solvent molecules. Broadly speaking, there is a correlation between them except for some irregularity in the solvents with a low polarity. In Figs. 13 and 14, $(F_{0i}d_i/d_{0i} - F_i)/F_{i500}$ and F_i/F_{i500} are plotted against K_C. These two figures suggest that solvents can be classified into two groups, one with a low polarity from cyclohexane to ether type compounds (1 to 5), and the other with a higher polarity from ethyl acetate to N, N-dimethylformamide (from 6 to 9). Hereafter these two groups will be denoted as group 1 and group 2.

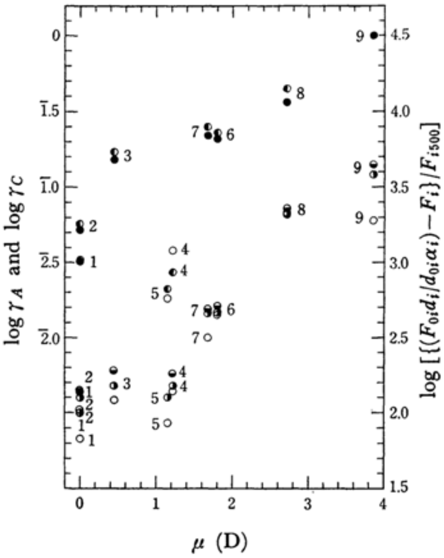

Fig. 12. $\log\gamma$ and $\log[\{(F_{0i}d_i/d_{0i}\alpha_i) - F_i\}/F_{i500}]$ vs. μ.

● log γ_{Ci}
◐ log γ_{Ai}
○ $\log[\{(F_{0i}d_i/d_{0i}\alpha_i) - F_i\}/F_{i500}]$ [MB] : 0.81 M
◑ $\log[\{(F_{0i}d_i/d_{0i}\alpha_i) - F_i\}/F_{i500}]$ [MB] : 1.60 M
◒ $\log[\{(F_{0i}d_i/d_{0i}\alpha_i) - F_i\}/F_{i500}]$ [MB] : 2.40 M
1 cyclohexane, 2 benzene, 3 p-dioxane, 4 isopropyl ether, 5 ethyl ether, 6, ethyl acetate, 7 tetrahydrofuran, 8 acetone, 9 dimethylformamide

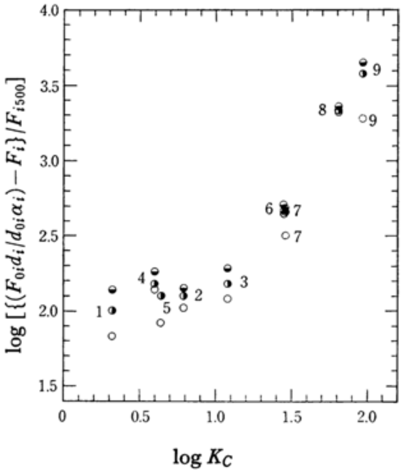

Fig. 13. log [{$(F_{0i}d_i/d_{0i}\alpha_i)-F_i\}/F_{i500}$] vs. log K_C.
● [MB] : 0.801 M, ○ [MB] : 1.60 M,
◑ [MB] : 2.40 M
1 cyclohexane, 2 benzene, 3 *p*-dioxane, 4 isopropyl ether, 5 ethyl ether, 6 ethyl acetate, 7 tetrahydrofuran, 8 acetone, 9 dimethylformamide.

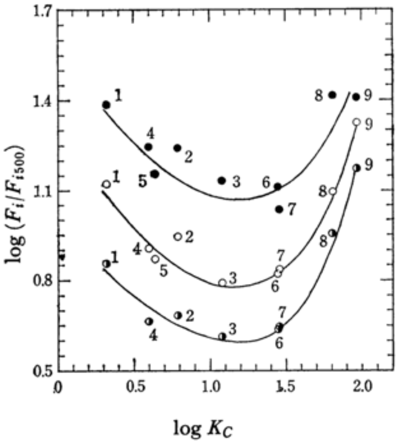

Fig. 14. log F_i/F_{i500} vs. log K_C plot.
● [MB] : 0.801 M, ○ [MB] : 1.60 M,
◑ [MB] : 2.40 M
1 cyclohexane, 2 benzene, 3 *p*-dioxane, 4 isopropyl ether, 5 ethyl ether, 6 ethyl acetate, 7 tetrahydrofuran, 8 acetone, 9 dimethylformamide

These two types of behaviour, as well as the results in Fig. 12, can well be comprehended on the basis of Weller's scheme for quenching. According to it, the quenching in nonpolar solvents is related to the formation of the CT complex, whereas the quenching in polar solvents occurs through the formation of radical ions. Plausible schemes for the two types of solvents are as follows:[5]

A) In nonpolar solvents

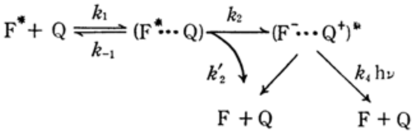

and

B) in highly polar solvents

$$\mathrm{F}^* + \mathrm{Q} \underset{k_{-1}}{\overset{k_1}{\rightleftarrows}} (\mathrm{F}^*\cdots\mathrm{Q}) \underset{k_3}{\rightarrow} \mathrm{F}^- + \mathrm{Q}^+$$

Thus, in nonpolar solvents an encounter complex (F*···Q) which has, more or less, a CT character, has two alternative paths, denoted by k_{-1} and k_2 or k_2'; their magnitudes depend upon the solvent, but usually $k_{-1}>k_2, k_2'$. $(\mathrm{F}^-\cdots\mathrm{Q}^+)^*$, which is reached by the k_2 path, is a stable CT complex capable of emission; its emissivity depends on the environment. k_2', which was included for the sake of generality, denotes another process of deactivation which occurs during the course of CT complex formation. On the other hand, an encounter complex in the highly-polar solvents, being quite a different type from that in nonpolar solvents, proceeds mainly along k_3 instead of k_2 and forms free ionic species. In the solvents with medium polarity, the k_2 and k_3 processes may compete with each other.

If one assumes, as is plausible, that the quenching efficiency in scheme A is far less than in scheme B, then the general tendency seen in Fig. 12 may be easily interpreted. Further, it is natural to consider that the A scheme prevails for group 1, whereas scheme B becomes gradually predominant for group 2. The analysis on the basis of the above scheme, however, requires much more data than those obtained above.

Below we will give only the plausible interpretation of the results shown in Figs. 9, 10, 13 and 14 by introducing a CT emission probability, ϕ_{CT}, which gives a ratio between the CT emission and the effective collisional quenching. Assuming Stern-Volmer's equation, the following relations can easily be derived:

$$F_{500}=\frac{Z\gamma[\mathrm{Q}]\phi_{\mathrm{CT}}}{k_f+k_d+k_{q\mathrm{O}_2}[\mathrm{O}_2]+Z\gamma[\mathrm{Q}]} \tag{6}$$

$$\frac{F_{500}}{F}=\frac{Z\gamma[\mathrm{Q}]\phi_{\mathrm{CT}}}{k_f} \tag{7}$$

$$\frac{F_0-F}{F_{500}}=\frac{k_f\tau_0}{\phi_{\mathrm{CT}}} \tag{8}$$

From Eq. 8, F_0-F/F_{500} or, more rigorously, $(F_0d_i/d_{0i}-F_i)/F_{i500}$ should depend merely on ϕ_{CT}. The slight dependence of ϕ_{CT} on [MB], as seen in Fig. 9, may perhaps be due to the quenching of the CT complex by MB. Alternatively, it may be due to the inadequeacy of the Stern-Volmer relation. Putting approximately $k_f\tau_0\approx$

---

[5] Cf. Ref. 3.

1, the solvents belonging to group 1 have ϕ_{CT} values ranging from 0.5×10^{-2} to 2×10^{-2}, whereas the solvents in group 2 have ϕ_{CT} values of $<0.5\times10^{-2}$. As may be seen from Fig. 13, ϕ_{CT} generally decreases with K_C; in group 1 it decreases very little, while in group 2 it decreases to a large extent.

The results in Fig. 14 and 10 can now be interpreted by means of Eq. 7. Thus in group 1, $Z\gamma$ increases while ϕ_{CT} decreases with the polarity, but since the former effect outweighs the latter, F_i/F_{500} decreases, as may be seen in Fig. 14. In group 2, on the other hand, the effect of the decrease in ϕ_{CT} predominates, since the increase of $Z\gamma$ is not so great (the maximum value of γ is 1); as a result, F_i/F_{500} again increases. The rather good linearity holding for the plots in Fig. 10 (as compared with Figs. 6, 7 and 8) may perhaps be due to the ϕ_{CT} factor, which decreases with the concentration of MB.

Thus, all the results can be interpreted if one assumes that, in group 1, $Z\gamma$ increases whereas ϕ_{CT} decreases a little with the polarity, and that in group 2 $Z\gamma$ increases and ϕ_{CT} decreases remarkably. These assumptions are quite natural in view of schemes A and B. It is not possible, however, to decide quantitatively how the contributions of schemes A and B depend upon the solvent polarity, and nor to decide how each elementary reaction in scheme A is influenced by the solvent polarity.

In summary, it may be said that in group 2 the formation of radical ions becomes easier with the solvent polarity, and that this is the main cause of the high quenching efficiency and the low CT emission. Although in group 1, the CT emission seems to become more easily observable with the polarity of the solvent, this is most probably due to the increase in γZ; the probability of the CT emission itself seems to decrease a little with the solvent polarity. The latter remark, however, must be further scrutinized in view of the irregular behavior to be seen in Fig. 12. The influence of the solvent polarity upon the emissivity of CT complex awaits further study.